Supporting Information

Monodispersed flower-like MXene@VO_2 clusters for aqueous zinc ion battery with superior rate performance

Zhibin Xu,[a] Xilong Li,[a] Yueang Jin,[a] Qi Dong,[a] Jiajia Ye,[a] Xueqian Zhang*[b] and Yitai Qian*[a]

[a]School of Chemistry and Material Science, University of Science and Technology of China, Hefei 230026, China

[b]School of Physics and Materials Engineering, Hefei Normal University, Hefei 230621, China.

1. Experimental Section

Synthesis of $Ti_3C_2T_x$ MXene nanosheets: $Ti_3C_2T_x$ MXene nanosheets were prepared as previously reported. Briefly, 5 g Ti_3AlC_2 MAX particles were added into a 100 mL hydrochloric acid (HCl, 12 M) solution containing 5 g lithium fluoride (LiF) and the suspension was stirred at 40 ℃ for around 45 h. The multi-layered MXene (m-MXene) was collected by centrifugation, which was then washed with deionized water several times until the supernatant was virtually neutral, before freeze-drying. MXene nanosheets were subsequently obtained by ice-water bath ultrasonic process. In detail, 1 g m-MXene was mixed with 100 mL deionized water before being ultrasonically treated for 1 h. MXene nanosheets were produced by centrifuging the suspension of m-MXene at 3500 rpm for 1 h and then freeze-drying the supernatant.

Preparation of MXene@VO_2 composite: Firstly, 1.2 g V_2O_5 and 1.8 g $H_2C_2O_4 \cdot 2H_2O$ were dissolved in 40 mL deionized water with continuous stirring at 75 ℃ for 1 h. Then, a predetermined amount of as-prepared MXene nanosheets (54 mg, 10 wt.%) was added to the fore prepared suspension and stirred until complete dispersion with N_2 purging to eliminate the dissolved O_2 to prevent the oxidation of MXene nanosheets in the subsequent hydrothermal procedure. Afterward, the suspension was sealed into a 50 mL Teflon-lined autoclave and kept in an oven at 180 ℃ for 3 h. After the autoclave was cooled down to room temperature, the final product was collected by centrifugation, washed multiple times with deionized water, and freeze-dried, named MXene@VO_2. For comparison, pure VO_2 was synthesized via the same method but without the addition of MXene nanosheets.

Materials characterization: The phase compositions of the samples were determined by X-ray diffraction (XRD) using a Philips X' Pert Super diffractometer with Cu K_α (λ=1.54 Å) over a 2θ range of 10-60°. To observe the microstructures and morphologies of the samples, scanning electron microscopy (SEM, JEOL-JSM-6700F), transmission electron microscopy (TEM, Hitachi H7650) and high-resolution transmission electron microscopy (HRTEM, JEM-2100F) was used, in conjunction

with energy dispersive spectroscopy (EDS) to analyze chemical element composition. The Raman spectrum was acquired by a JYLABRAM-HR Confocal Laser Micro-Raman spectrometer at 532 nm. The X-ray photoelectron spectroscopy (XPS) results were collected on a Perkin-Elmer ESCALAB 250 X-ray photoelectron spectrometer to analyze the chemical structures and elemental valence states. The surface areas of the samples were obtained by a physisorption analyzer (ASAP-2020) based on N_2 adsorption-desorption.

Electrochemical measurements: To measure the electrochemical performances of the samples, the CR2032 coin cells were fabricated, which included the cathode, anode (100 μm, zinc foil), electrolyte (200 μL, 2 M ZnOTf) and separator (GF/D glass fiber membrane). Therein, the cathode was prepared by uniformly mixing the active materials (VO_2, MXene@VO_2), super P, and PVDF in a mass ratio of 70%:20%:10% and then mixing with *N*-methyl-2-pyrrolidone (NMP), after which the slurry was coated on the current collector (titanium mesh) followed with drying in a vacuum oven. The mass load of the active materials is about 3.0 mg cm^{-2} on each electrode. The cyclic voltammetry (CV) and electrochemical impedance spectroscopy (EIS) were tested on an electrochemical workstation (CHI660E). The galvanostatic charge/discharge (GCD) tests were conducted by battery testing systems (LAND CT3001A) to acquire the cycle and rate performances of the samples. The self-charging battery is prepared through similar assembling procedure of 2032 cells with the MXene@VO_2 composite as the cathode, 2 M ZnOTf as the electrolyte and Zn metal plate as the anode. What is different is that the cathode is exposed to the air.

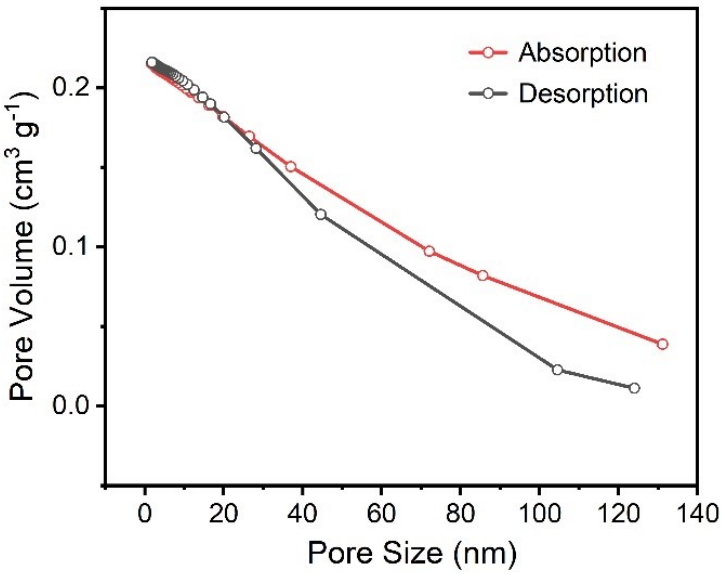

Figure S1. The BJH pore size distribution curves of MXene@VO_2 composite.

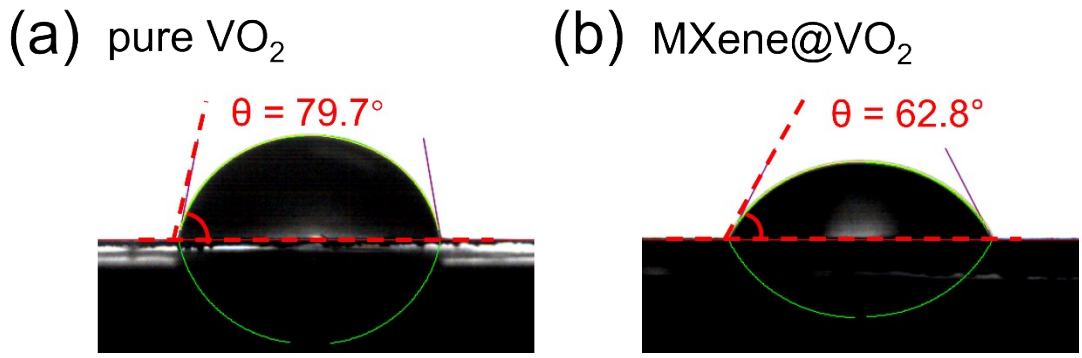

Figure S2. The contact angle of pure VO_2 and MXene@VO_2 with 2 M ZnOTf electrolyte.

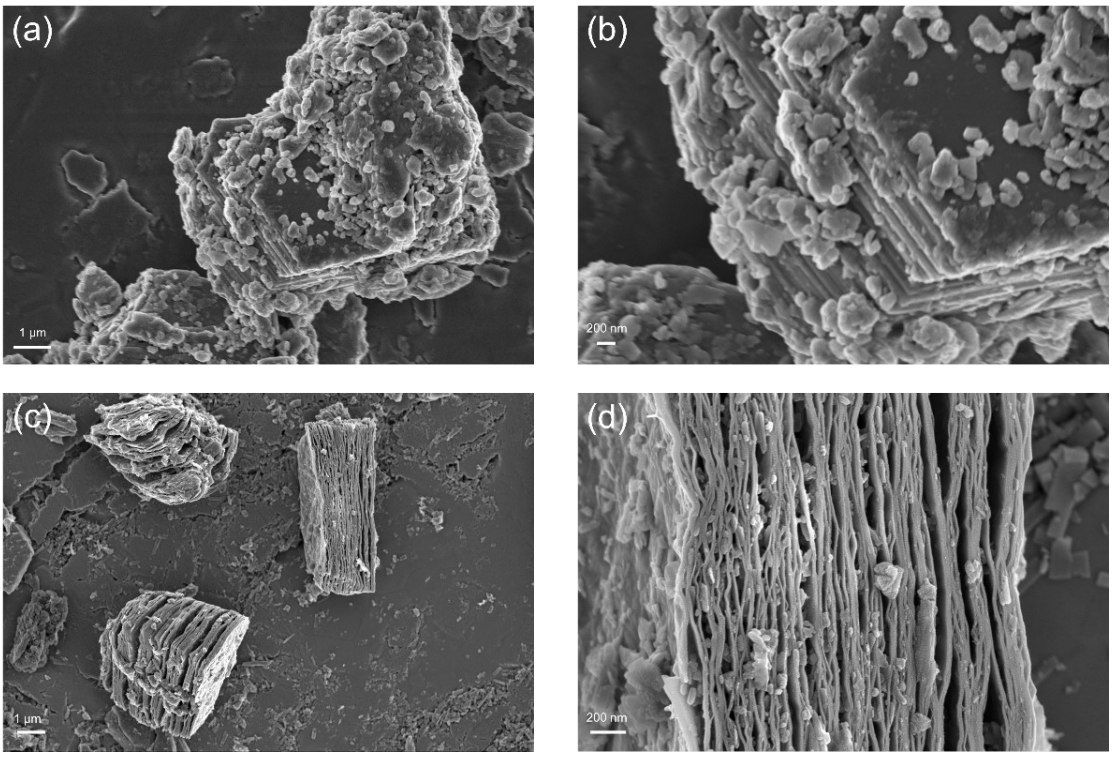

Figure S3. SEM images of (a,b) MAX and (c,d) m-MXene at different magnifications.

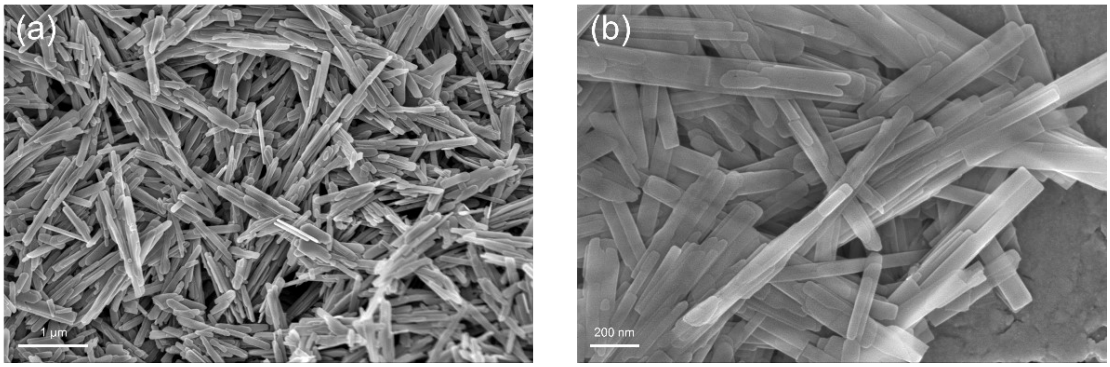

Figure S4. SEM images of pure VO_2 at different magnifications.

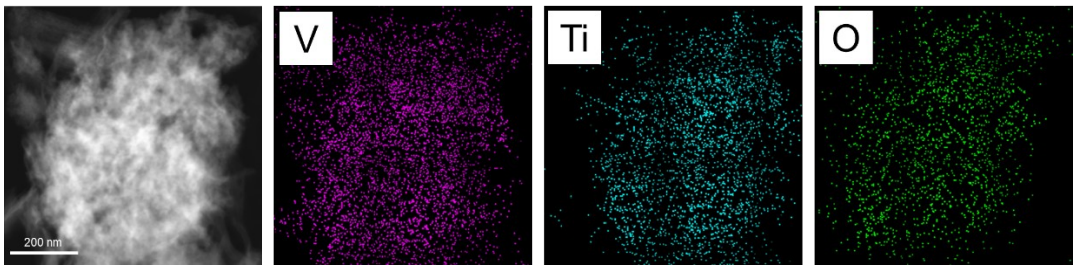

Figure S5. TEM image of MXene@VO_2 and corresponding EDS mappings of V, Ti, O elements.

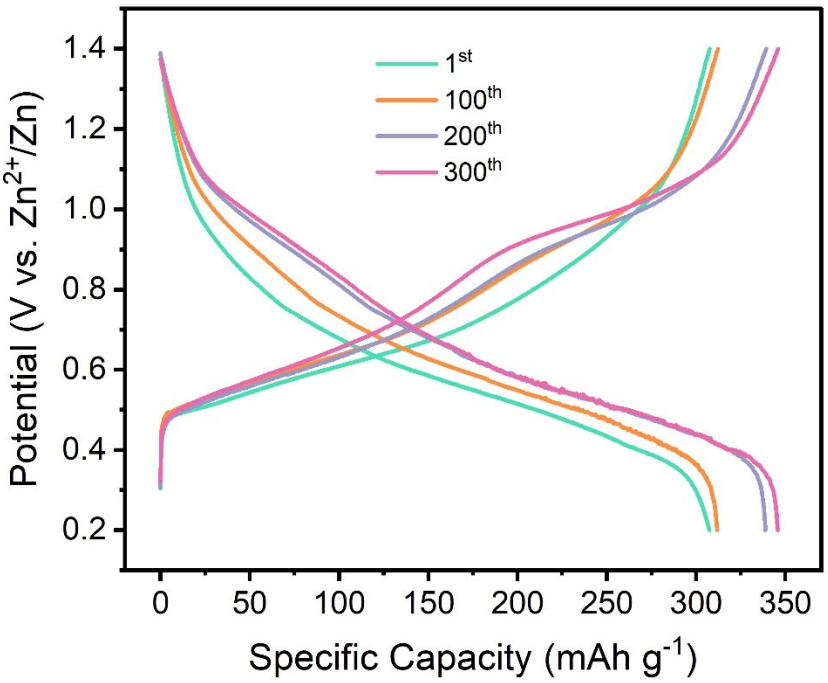

Figure S6. Galvanostatic charge/discharge curves of the MXene@VO_2 composite at 0.5 C.

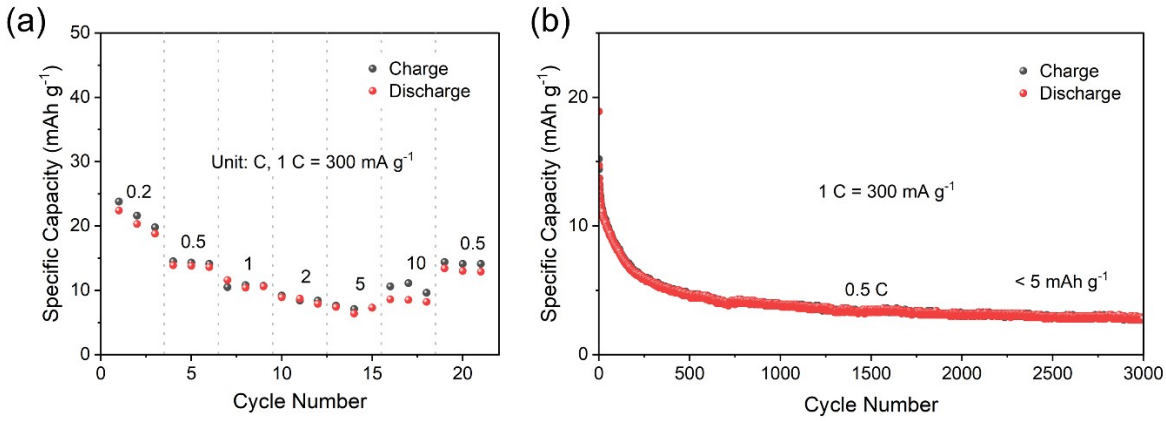

Figure S7. The rate and cycle performances of MXene.

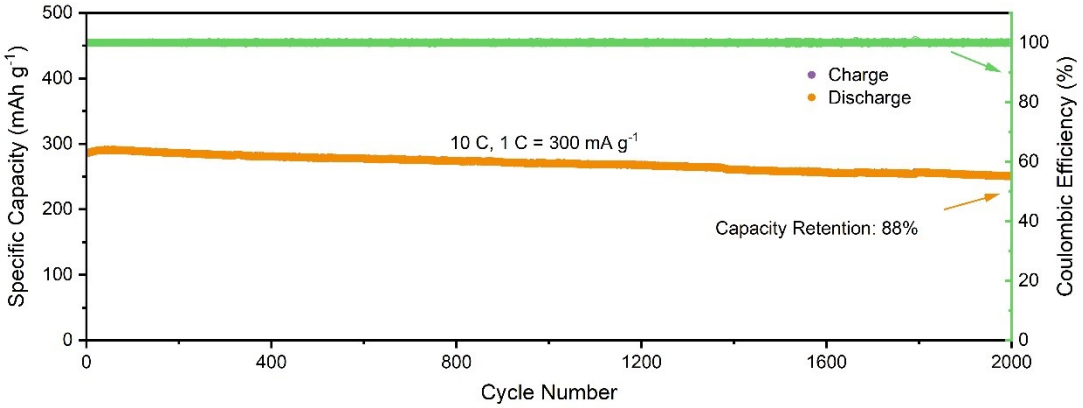

Figure S8. The cycle performance of MXene@VO_2 at 10 C.

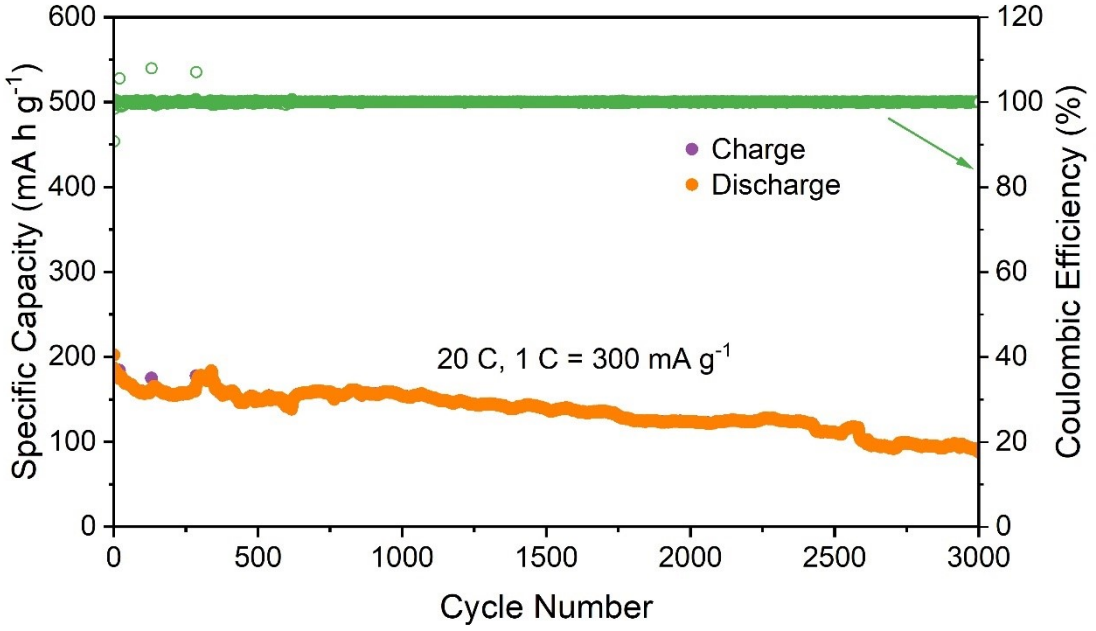

Figure S9. The cycle performance of pure VO_2 at 20 C.

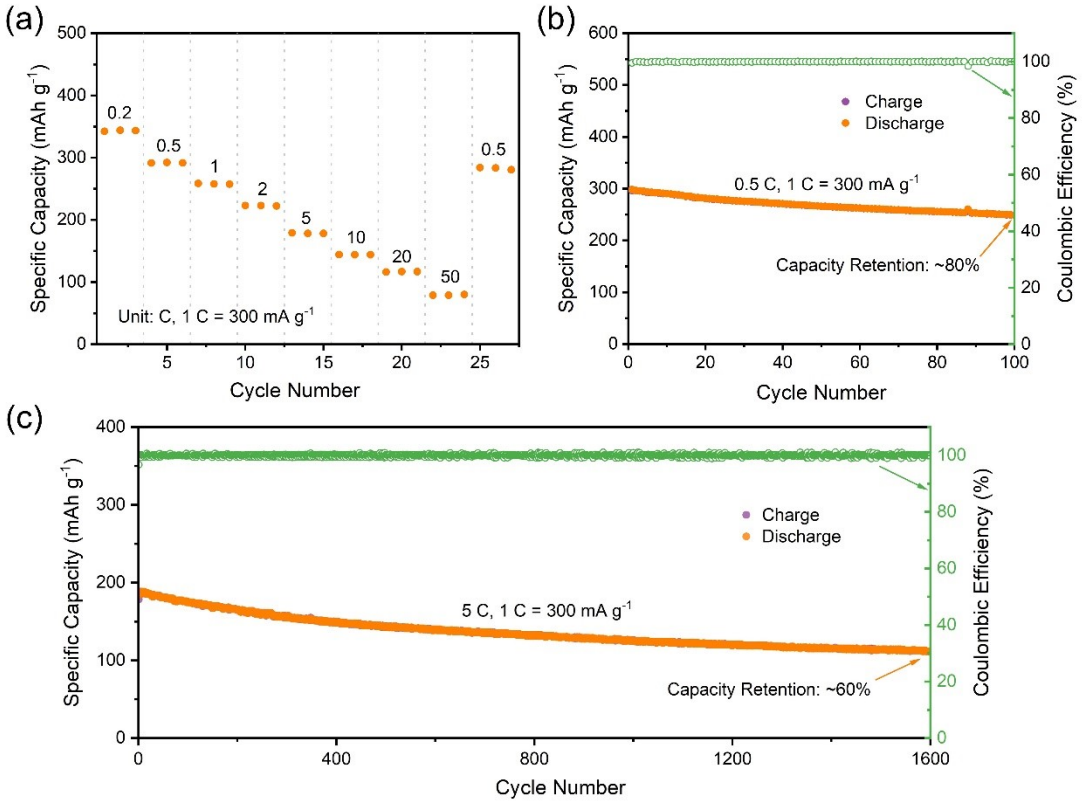

Figure S10. The electrochemical performance of MXene@VO_2 at -20 °C: (a) The rate performance. (b,c) The cycle performance at (b) 0.5 C and (c) 20 C.

The low-temperature performance of MXene@VO_2 composite used as the cathode of AZIB was further measured at -20 °C in a low-temperature test chamber. MXene@VO_2 offers a capacity of about 300 mA h g^{-1} at 0.5 C, with a capacity retention of 80% over 100 cycles. Figure S9b exhibits the rate performance of MXene@VO_2, which possesses a capacity of 291.5, 258.6, 223.0, 179.1, 144.2, 116.7 mA h g^{-1} at 0.5 C, 1 C, 2 C, 5 C, 10 C and 20 C respectively. The capacities at low rates are close to those at room temperature, demonstrating the superior low-temperature performance of MXene@VO_2. However, when the rate is adjusted to 50 C, MXene@VO_2 only offers a capacity of 79.9 mA h g^{-1}, which can be ascribed to the low ion conductivity at low temperature leading to the slight deterioration of high-rate performance. The long-term cycle performance of MXene@VO_2 at -20 °C can be obtained from Figure S9c, which possesses an initial capacity of about 190 mA h g^{-1} at 5 C with a capacity decay of 0.025% per cycle and a coulombic efficiency of about 100% over 1600 cycles.

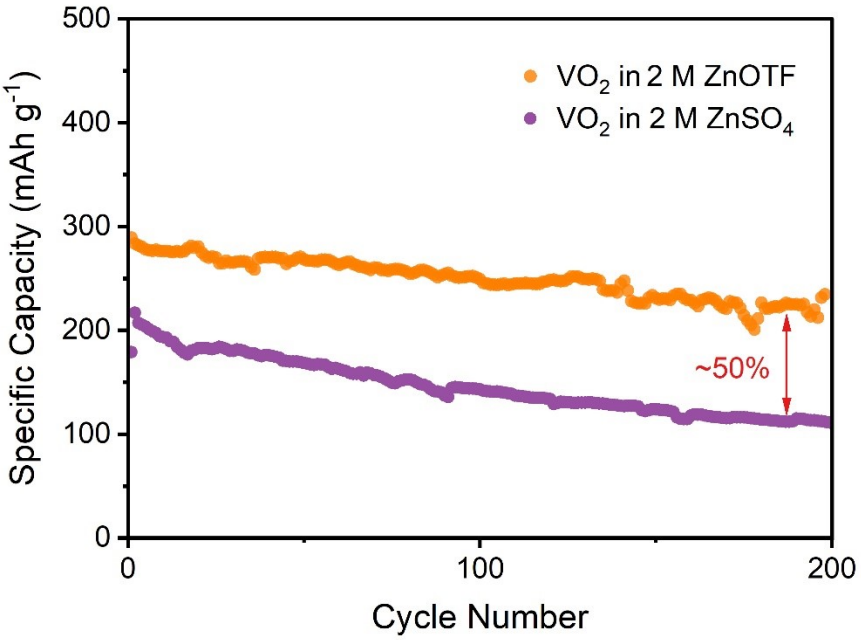

Figure S11. The electrochemical performance of MXene@VO_2 in different electrolytes.

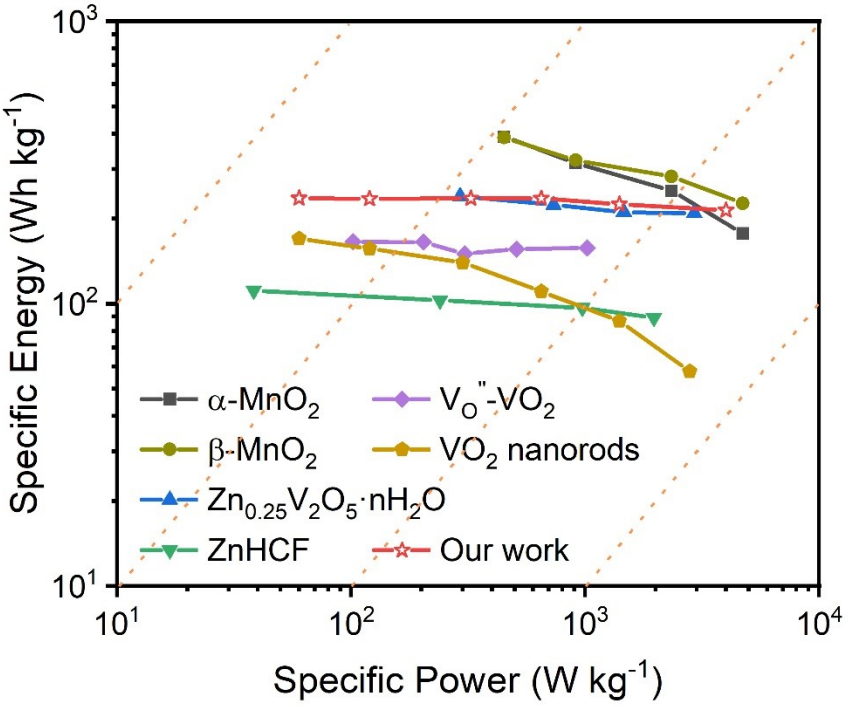

Figure S12. The Ragone plots of MXene@VO_2 compared with other reported cathodes for AZIBs.

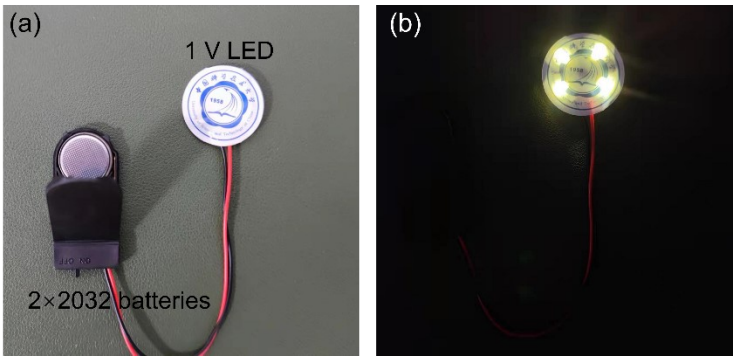

Figure S13. The photographs of lighting 1V LED bulb using two 2032 cells (MXene@VO_2 as cathode).

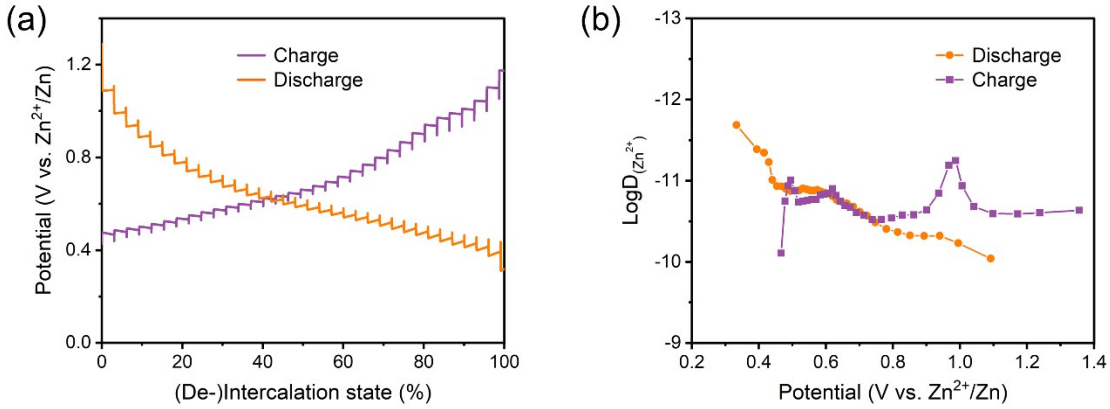

Figure S14. (a) The galvanostatic charge/discharge curves of GITT test at 0.2 C (work for 10 min and rest for 60 min). (b) The diffusion coefficient of Zn^{2+} in the MXene@VO_2 electrode.

Table S1. The comparison of various vanadium dioxide-based materials and their electrochemical performances in AZIBs.

Cathode	Electrolyte/ Potential window	Rate performance	Cycling performance (Capacity retention)	Ref.
MXene@VO_2	2 M ZnOTf 0.2-1.4 V	363.6 mA h g^{-1} at 0.2 C 289.1 mA h g^{-1} at 10 C 169.1 mA h g^{-1} at 50 C	76% over 5000 cycles at 20 C	Our work
TiC_x@VO_2	2 M ZnOTf 0.4-1.6 V	378.8 mA h g^{-1} at 1 A g^{-1} 303.1 mA h g^{-1} at 20 A g^{-1}	82% over 2600 cycles at 20 A g^{-1}	1
VO_2@MXene film	2 M ZnOTf 0.3-1.3 V	228.5 mA h g^{-1} at 0.2 A g^{-1} 158.3 mA h g^{-1} at 2 A g^{-1}	72.1% over 2500 cycles at 5 A g^{-1}	2
V_2O_x@V_2CT_x	1 M $ZnSO_4$ 0.3-1.6 V	304 mA h g^{-1} at 0.05 A g^{-1} 107 mA h g^{-1} at 1 A g^{-1}	81.6% over 200 cycles at 1 A g^{-1}	3
VO_2 nanoflakes	1 M $ZnSO_4$ 0.2-1.0 V	289 mA h g^{-1} at 0.1 A g^{-1} 156 mA h g^{-1} at 2 A g^{-1}	74% over 2000 cycles at 2 A g^{-1}	4
VO_2 nanorods	1 M $ZnSO_4$ 0.2-1.2 V	325.6 mA h g^{-1} at 0.05 A g^{-1} 72 mA h g^{-1} at 5 A g^{-1}	86% over 5000 cycles at 3 A g^{-1}	5
VO_2 nanofibers	3 M ZnOTf 0.3-1.4 V	357 mA h g^{-1} at 0.1 A g^{-1} 171 mA h g^{-1} at 52.1 A g^{-1}	91.2% over 300 cycles at 0.2 A g^{-1}	6
VO_2 nanorods	1 M $ZnSO_4$ 0.2-1.3 V	384 mA h g^{-1} at 0.05 A g-1 272 mA h g^{-1} at 3.0 A g-1	75.7% over 950 cycles at 3 A g^{-1}	7
$VO^{\cdot\cdot}$-VO_2	3 M ZnOTf 0.4-1.5 V	375 mA h g^{-1} at 0.1 A g^{-1} 220 mA h g^{-1} at 5 A g^{-1}	85% over 2000 cycles at 5 A g^{-1}	8
VO_2(B)/RGO	3 M ZnOTf 0.2-1.4 V	456 mA h g^{-1} at 0.1 A g^{-1} 292 mA h g^{-1} at 10 A g^{-1}	90% over 1000 cycles 5 A g^{-1}	9

References

1. W. Kou, L. Yu, Q. Wang, Y. Yang, T. Yang, H. Geng, X. Miao, B. Gao and G. Yang, *J. Power Sources*, 2022, **520**.
2. Z. Shi, Q. Ru, Z. Pan, M. Zheng, F. Chi-Chun Ling and L. Wei, *ChemElectroChem*, 2021, **8**, 1091-1097.
3. R. Venkatkarthick, N. Rodthongkum, X. Zhang, S. Wang, P. Pattananuwat, Y. Zhao, R. Liu and J. Qin, *ACS Applied Energy Materials*, 2020, **3**, 4677-4689.
4. Q. Pang, H. N. Zhao, R. Q. Lian, Q. Fu, Y. J. Wei, A. Sarapulova, J. Q. Sun, C. Z. Wang, G. Chen and H. Ehrenberg, *J. Mater. Chem. A*, 2020, **8**, 9567-9578.
5. L. Chen, Y. Ruan, G. Zhang, Q. Wei, Y. Jiang, T. Xiong, P. He, W. Yang, M. Yan, Q. An and L. Mai, *Chem. Mater.*, 2019, **31**, 699-706.
6. J. Ding, Z. Du, L. Gu, B. Li, L. Wang, S. Wang, Y. Gong and S. Yang, *Adv. Mater.*, 2018, **30**, e1800762.
7. Z. L. Li, S. Ganapathy, Y. L. Xu, Z. Zhou, M. Sarilar and M. Wagemaker, *Adv. Energy Mater.*, 2019, **9**.
8. Z. Li, Y. Ren, L. Mo, C. Liu, K. Hsu, Y. Ding, X. Zhang, X. Li, L. Hu, D. Ji and G. Cao, *ACS Nano*, 2020, **14**, 5581-5589.
9. F. H. Cui, J. Zhao, D. X. Zhang, Y. Z. Fang, F. Hu and K. Zhu, *Chem. Eng. J.*, 2020, **390**.